Modeling of the electromagnetic forming of metal cans for optoelectronic components

D. LUCA*, V. SCHIOPU
Department of Technologies and Equipments for Materials Processing, Technical University, 700050 Iasi, Romania

A major interest regarding electromagnetic forming of metal results from the fact that, unlike all known forming methods, plastic deformation of the material is not produced by physical contact between a punch type tool and the workpiece, the desired shape being obtained by means of magnetic pressure. The main objective of this paper is to analyze the possibility of using electromagnetic forming to manufacture some metal cans for optoelectronic components (photodiodes, phototransistors). The paper presents a finite element model for electromagnetic forming of a TO-39 metal can. Finite element modeling was aimed to establish the main working electromagnetic and mechanical parameters that assure proper forming of the metal can, to help tools designing (coil and mandrel) and to establish relative positioning and fastening mode between workpiece and tools.

(Received April 9, 2015; accepted June 24, 2015)

Keywords: Photodiode, Metal can, Electromagnetic forming, Finite element modeling

1. Introduction

Metal forming processes cover an important area of the industrial production of metal components. The main purpose of a plastic deformation operation is to produce the desired change in shape and dimensions of a metal workpiece.

Metal forming is used for obtaining complex shaped parts with very large dimensions (that can reach several meters), but also very small ones with dimensions of a few millimeters, as are the metal cans (capsules) for optoelectronic components (e.g., photodiodes, photo-transistors, etc.).

This wide variety of plastically deformed parts is obtained by applying classical techniques (rolling, forging, die forging, extrusion, drawing, deep-drawing, etc.) or some unconventional forming methods (hydroforming, explosive forming, electrohydraulic forming, electromagnetic forming, etc.).

Electromagnetic forming (EMF) is a process applied to manufacture relative small parts through plastic deformation from workpieces in the form of metal sheet or tube (Fig. 1). The tube free bulging using expansion coil has been described in many papers.

The effects of various working conditions on tube bulging by electromagnetic forming were analytically and experimentally investigated [2]. Considering the influence obtained by changing the capacitance of capacitor bank and the length of solenoidal coil on the formed tube, the forming process efficiency was studied.

In reference [3], the finite element analysis has been used to investigate the effects of the coil and tube geometry, as well as the effects of the resistivity and length of the workpiece on the magnetic pressure in metal tube expansion.

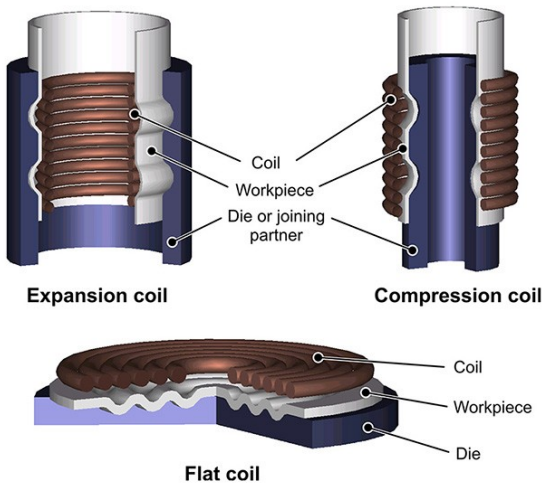

Fig.1. Basic variants of EMF process [1].

Electromagnetic forming was used as a test method to model the ductility of materials processed with high speed. The concept of forming limit diagrams used for quasi-static deformation was applied to study the ductility of aluminum alloy tubes free expanded by magnetic pressure [4].

The free electromagnetic tube bulging was studied in paper [5], where the time distribution of magnetic pressure on various length tubes was presented. Also, effect of tube size on the space distribution of radial and axial magnetic pressure was studied.

Methods enabling electromagnetic expansion of low conductive metal tubes were presented in reference [6]. The authors used the finite element method to calculate electromagnetic field coupled with mechanical deformation and temperature for low conductive metal tubes that were coated with highly conductive layers.

The paper [7] presents the experimental and simulation results of electromagnetic expansion of an aluminum alloy tube. The primary objective of the study was an accurate measurement of high velocity by Photon Doppler Velocimetry technique and comparison of experimental data with simulation performed by finite element method.

Also, free constriction of the tube using compression coil was presented in several papers. Karch and Roll [8] conducted a transient analysis of free compression aluminum tubes by electromagnetic forming. The numerical model developed can predict the electromagnetic field, the stresses and strains which occur during the forming process, and the temperature in the part created by eddy currents that passes through it (heating by Joule effect).

The effects of current frequency on electromagnetic tube compression had been studied by means of the sequential coupling simulation, using the finite element method [9, 10]. The optimum current frequency is one of the most basic requirements for a well done design of the EMF machine. In these conditions, maximum deformation can be achieved during electromagnetic forming.

The importance of ensuring optimal frequency of the discharge current for obtaining maximum deformation during electromagnetic forming was successively confirmed by other studies [11, 12].

The stress-strain state of a magnesium alloy tube was analyzed by electromagnetic forming tests and finite element simulations in reference [13].

The authors demonstrated that the causes of oblique and longitudinal cracks of tube were inhomogeneous distributions of the normal stress in the axial and circumferential directions.

A compression process by electromagnetic forming of high strength steel tubes has been studied both experimentally and numerically in [14]. Performed experiments have shown that by reducing the capacitance of the capacitor bank, the rising time of the pressure pulse can be minimized which reduces the tendency of bucking the tubes.

In paper [15], the effect of tube thickness and the field shaper's geometry on the magnetic force, the deformation characteristics of the tube of aluminum and the produced mechanical stress or strain rate during electromagnetic tube compression were investigated through simulations based on the finite element method.

The simulation of electromagnetic compression forming was performed also in paper [16] applying the finite element analysis, for steel tubes, using a helical actuator (solenoidal coil) and different energy levels.

Fewer papers presents cases of net shape parts obtained from tubular workpieces by electromagnetic expansion or compression.

One of these papers [17] carries out a numerical simulation of magnetic pressure acting on the tube under the influence of die. The analysis model was created by means of finite element method for electromagnetic tube expansion with die.

Electromagnetic compression of the tubes was used as a method of joining two components with light weight [18]. Radial pressure applied to tubular workpieces causes a uniform reduction of the diameter and a very good permanent joining is obtained.

Nowadays, many of the researches performed in field of optoelectronics are focused on the introduction of some advanced materials and new methods for manufacturing photodiodes and phototransistors, and metal cans should provide a good mechanical protection for these optoelectronic devices but, in the same time, the manufacturing costs should be reduced as much as possible.

In article [19] is reported the achieving of a highly crystalline thin layer of 1-aminoanthracene compound onto the glass substrate using hot wall technique. Photoluminescence tests showed prominent green emission peak at this thin film. A material of perspective, with possibilities of application in field effect thin films transistors and optoelectronic devices, is polymethylmethacrylate (PMMA) [20]. Authors of the paper [21] reports that photodiodes based on the heterojunction n-InGaZnO/p-Si have been made, using the method of radio frequency magnetron sputtering of n-IGZO thin films on p-type Si(100) substrates. A photo response under the influence of irradiation with visible light, was obtained at a junction formed of a thin film of nickel phthalocynanine (NiPc) deposited on the aluminum (previously deposited on the glass substrate) by the vacuum evaporation method [22].

In the present paper, considering the transient phenomena occurring at the discharge of the capacitor bank and the workpiece material properties, working conditions were established for electromagnetic forming of the metal can TO-39 with circular window, used for encapsulate optoelectronic devices like photodiodes/ phototransistors and LED-s. This type of optoelectronic components are made of semiconductor materials in which, in the case of photodiodes and phototransistors, the reverse current varies with illumination. These devices are used for the conversion of optical signals to electrical signals or vice-versa (LED-s). For mechanical protection of photosensitive element, it is encapsulated in plastic, ceramic, glass or metal cans.

Transistor outline (TO) housings are now standard in optoelectronics. For decades, they have been used to package semiconductor chips and are available in standard sizes.

These chips used as transmitters or receivers of light signals are reliably protected by the TO housings. TO housings generally consist of a round base with glass-to-metal feedthroughs that allow electrical signals to enter into the housing.

The optoelectronic chip is fixed to the base and the package is sealed with a metal cap provided with a round window that allows light signals to enter. The window is sealed with glass lenses or discs soldered to the caps.

Usually, the metal cans are made from Fe-Ni-Co alloys such is kovar (ASTM F15 alloy) specially designed to match the expansion characteristics of borosilicate glasses and alumina ceramics in order to allow direct

mechanical connections over a range of temperatures. Aluminum and cooper alloys are also used.

In the present paper, in both finite element method (FEM) analysis and experimental tests, two kind of metal tubes are used as workpieces, first from Aluminum 99.5 (Al 1050) and second from brass (nickel coated on the external surface).

2. Setup description and model formulation

Electromagnetic forming is an efficient and yet underutilized process for forming or joining metal sheets and tubes.

The main elements of an EMF system (Fig. 2) are as follows:

- T - transformer, supplied from a source of alternating current, raise the charging voltage of the capacitors up to ten thousand volts or even more;
- R - rectifier, responsible for capacitor bank charging in continuous current;
- C - capacitor bank, which ensure the storage of required energy to be discharged;
- S_1 - charging switch;
- S_2 - spark gap, considered as a high current fast closing switch for the discharge circuit;
- 1 - compression coil, the working tool of the system (together with the mandrel), through which the high current i_1 passes at discharge of the capacitor bank, thus resulting the active magnetic field;
- 2 - workpiece, a tube, traversed by induced current i_2, which is to be shaped after a given configuration of a mandrel 3.

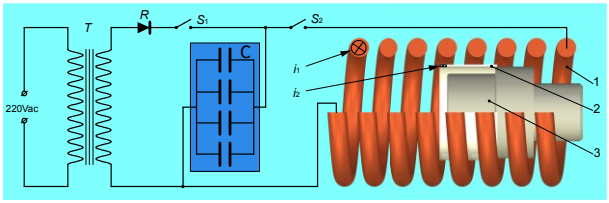

Fig. 2. The EMF system for tube compression.

The most important parameters, in the case of manufacturing parts by electromagnetic forming, are the discharge current i_1 that passes through the coil and the magnetic flux density B produced by the coil, according to the relationships:

$$i_1(t) = I_0 \cdot \mathrm{e}^{-\alpha t} \sin \omega t \tag{1}$$

$$B(t) = B_0 \cdot \mathrm{e}^{-\alpha t} \sin \omega t \tag{2}$$

where I_0 is the maximum value (amplitude) of the discharged current, α represents the damping coefficient, of magnetic flux density.

Considering that the discharging circuit is of RLC type, the maximum magnitude of the discharged current can be determined with the expression:

$$I_0 = V\sqrt{\frac{C}{L}}\left(1-\frac{\pi R}{4}\sqrt{\frac{C}{L}}\right) \tag{3}$$

where V is the charging voltage of the capacitor bank, C represents the total capacitance of the capacitor bank, L is the total inductance of the discharge circuit and R is the total resistance of the discharge circuit.

The damping coefficient α and the current pulsation ω are determined with the relationships:

$$\alpha = \frac{R}{2L} \tag{4}$$

$$\omega = \sqrt{\frac{1}{LC}-\left(\frac{R}{2L}\right)^2} \tag{5}$$

The maximum value of the magnetic flux density can be determined by relationship:

$$B_0 = \frac{\mu_0 N I_0}{L_s} \tag{6}$$

where μ_0 is the magnetic permeability of vacuum, N is the solenoid number of windings and L_s is the solenoid length.

Besides the discharge current intensity, a decisive influence on the electromagnetic forming process has the discharge current frequency, which is determined with the relationship:

$$f = \frac{1}{2\pi}\sqrt{\frac{1}{LC}-\frac{R^2}{4L^2}} \tag{7}$$

The discharge current frequency directly influences the deformation degree, there being an optimal frequency value for which the maximum deformation degree is obtained.

The total pressure acting on the part is equal with the pressure difference on its two faces:

$$p = \frac{1}{2}\mu_0 (H_1^2 - H_2^2) \quad [\mathrm{Pa}] \tag{8}$$

where H_1 [A/m] is the magnetic intensity in the space between solenoid and workpiece and H_2 [A/m] is the magnetic intensity on the opposite (inside) face of the workpiece.

3. Finite element modeling

In this paper, a 3D model is set up using loose coupling method between transient electromagnetic problem and dynamic mechanical problem of the electromagnetic forming process.

In finite element modeling of electromagnetic forming processes of metals, great importance has the analysis of the electromagnetic field created in the workspace between the tool (coil) and the workpiece. Electromagnetic field analysis includes a wide range of problems in engineering and physics, being governed by laws that can be expressed very concisely by a single set of equations called Maxwell equations [23], [24]. Maxwell equations can be written using differential operators as follows [25]:

$$\text{rot}\, E = -\partial B / \partial t \tag{9}$$

$$\text{rot}\, H = J \tag{10}$$

$$\text{div}\, J = 0 \tag{11}$$

$$\text{div}\, B = 0 \tag{12}$$

where, E [V/m] is the electric field; B [T] represents magnetic flux density; H [A/m] is the magnetic intensity; J [A/m^2] is the current density and t [s] is the time. The first three equations are called evolution equations and the equation (12) represents equation of state. To these differential equations are added the constitutive equations expressed by:

$$J = \text{f}(E,B) = \sigma_w (E + v \times B) \tag{13}$$

$$B = \text{f}(H) = \mu H \tag{14}$$

where σ_w is the electrical conductivity of the workpiece, v represents velocity and μ is the magnetic permeability.

The basic properties of the materials from model are given in Table 1.

Table 1. Properties of materials used in EMF process

Workpiece (Al 1050)	Relative permeability	1.00002
	Resistivity	2.81×10^{-8} Ω·m
	Density	2.71×10^{3} kg/m^3
	Yield strength	35 MPa
	Ultimate strength	90 MPa
	Young's modulus	69 GPa
	Poisson's ratio	0.33
Coil (Cooper)	Relative permeability	0.99999
	Resistivity	0.0178×10^{-6} Ω·m
Mandrel	Relative permeability	1.00 (PTFE)
Air	Relative permeability	1.00

Due to the helical form of the coil, the geometry of the process is not fully symmetrical, and a 3D model is required. However, most of the researchers used axisymmetric models in their FEM simulation for reasons of time consuming. In this research, both 3D and axisymmetric models were used.

The transient electromagnetic forming model consists of air region, workpiece, mandrel and coil and it was built in following hypotheses:

- the coil current is distributed uniformly in the wire cross-section;
- the permeability and conductivity of materials are constant and isotropic;
- the influence of temperature variation is neglected.

A detail image of the finite element mesh for the electromagnetic forming model is shown in Fig. 3, in quarter section view.

The interaction of the magnetic fields from the coil and the workpiece creates body forces on both the workpiece and the coil. Lorentz's law governs the generation of these forces:

$$F = \int_v f_v \, \text{d}v = \int_v \left(J \times B \right) \tag{15}$$

where f_v is the volumetric force density.

The Lorentz's forces field acting in the workpiece volume, obtained from electromagnetic simulation, is then transferred to dynamic mechanical simulation.

In the mechanical simulation phase, the strain-rate hardening effect, occurring in the workpiece material, was considered by means of the Cowper-Symonds constitutive model [27]:

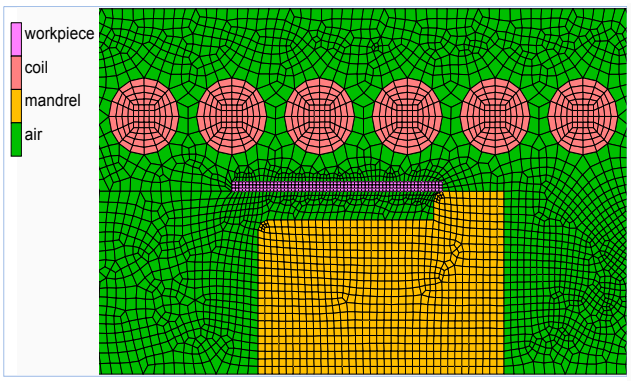

Fig. 3. Detail of quarter section view of finite element mesh.

$$\sigma = \sigma_y \left[1 + \left(\frac{\dot{\varepsilon}}{C} \right)^p \right] \tag{16}$$

where σ_y is the quasi-static yield strength [MPa], $\dot{\varepsilon}$ is the plastic strain rate [s^{-1}], C = 6500 s^{-1} and p = 0.25 are specific parameters for aluminum.

The proposed metal can to be manufactured by electromagnetic forming have the shape and dimensions shown in Fig. 4, according to JEDEC standard. Traditionally this part is obtained by mechanical deep-drawing and punching from metal sheet and due to circular

form of the workpiece, a significant surface of the raw material is wasted.

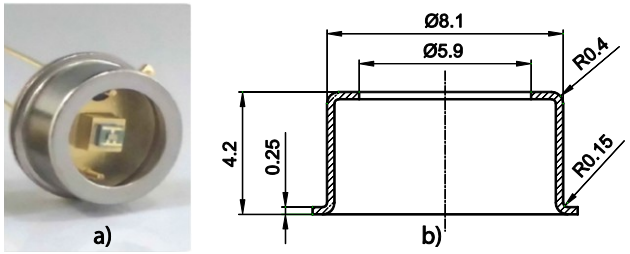

Fig. 4. The metal can TO-39: a) UV emitter MTE-F13 (MARKTECH); b) Dimensions of TO-39 can [26].

Table 2. Dimensions and circuit parameters

Coil	Internal diameter	$12^{+0.1}$ mm
	Coil length	34.5 mm
	Wire cross-section diameter	2.2 mm
	Pitch	4 mm
	Number of turns	8
Workpiece	External diameter	$9.5^{-0,1}$ mm
	Length	6 mm
	Thickness	0.25 mm
Circuit parameters	Discharged energy	2.5 kJ
	Circuit resistance	10.89 mΩ
	Circuit inductance	1.84 µH
	Capacitance	200 µF

The forming tool for tube compression is an external solenoidal coil made of copper wire with 2.2 mm diameter and a pitch of 4 mm. The workpiece is a tube of aluminum, with the dimensions given in Table 2, where are indicated the size of the coil and the discharge circuit parameters. The workpiece is formed over a mandrel made of insulating material (PTFE). The mandrel has a threaded section by means of which the axial position of the workpiece can be adjusted.

4. Results and discussions

For the given electrical circuit parameters of the electromagnetic forming equipment (Table 2), after the equivalent circuit simulation, the waveforms of discharge voltage and current were obtained. These amortized sine curves are in opposite phases and have the same time period $T = 116$ µs.

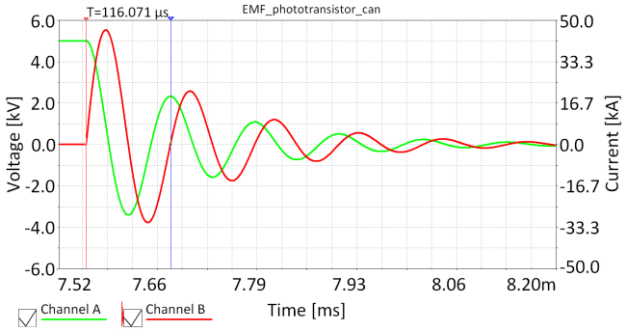

Fig. 5. Electrical circuit simulation: Discharge voltage and current waveforms.

The magnetic flux density distribution is shown in Fig. 6 in an YZ (axial) section of the 3D model. It can be observed that, around the workpiece, this distribution is not symmetric due to the non symmetry of the working tool (solenoidal coil).

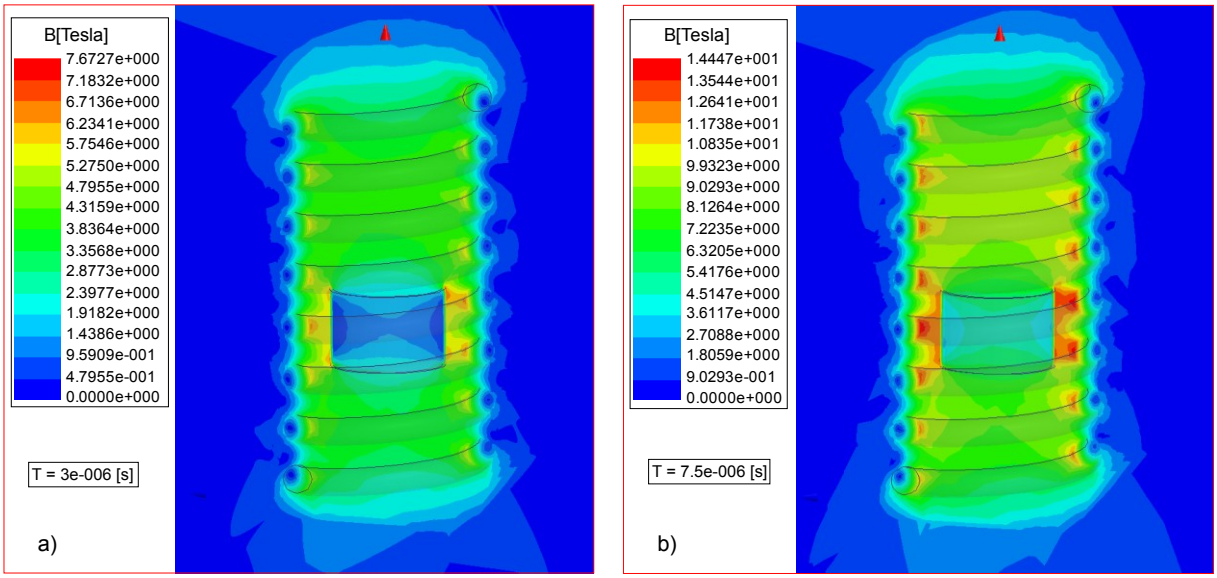

Fig. 6. Magnetodynamic finite element simulation. Distribution of magnetic flux density for two process moments: a) Time=3 µs; b) Time=7.5 µs.

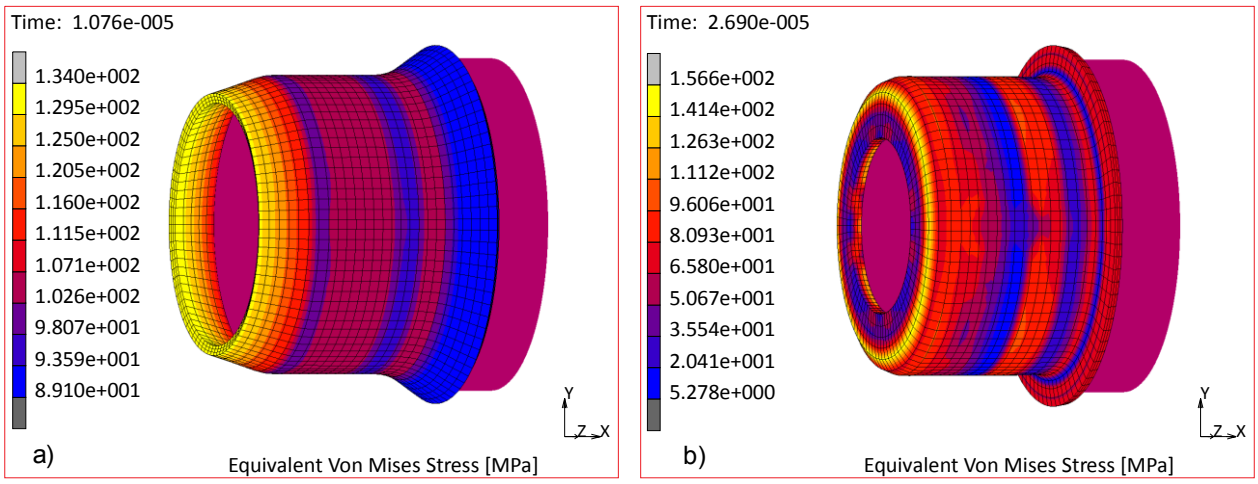

Fig. 7. Structural dynamic finite element simulation. Distribution of equivalent von Mises stress for two process moments: a) Time=10.76 μs and b) Time=26.90 μs.

It is known that a significant deformation in such forming processes occurs only in the first semi-period of the discharge current curve, and for this reason both electromagnetic and mechanical simulations are done for a total time of $T/2$ = 58 μs, in twenty intermediate steps.

The distribution of equivalent von Mises stresses in the workpiece during electromagnetic forming process is presented in Fig. 7 for two analysis time-steps.

By running iterative test of finite element analysis (varying charging voltage of capacitors, design parameters of coil and mandrel and relative positioning between tools and workpiece), aiming to obtain optimum stresses and strains distribution over the workpiece during deformation, the entire forming process optimization was attained.

The optimum working parameters for electromagnetic forming of TO-39 metal can are presented in Table 3.

Table 3. Working parameters for TO-39 metal can

Discharging current	58 kA
Discharging voltage	5 kV
Coil inductance	0.335 μH
RLC circuit period	116 μs
Average magnetic pressure	20 MPa
Maximum equivalent von Mises stress	220.6 MPa
Maximum equivalent plastic strain	0.8331

In Fig. 8 are presented the electromagnetic forming equipment used in this study and the coil designed and realized on the basis of data obtained from FEM simulation.

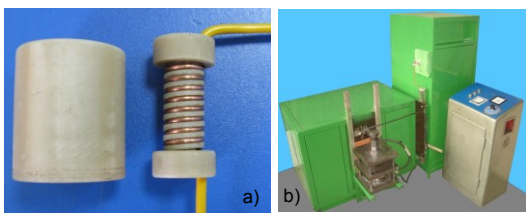

Fig. 8. Experimental setup: a) Coil assembly (coil housing - left); b) Electromagnetic forming equipment.

After the first set of experimental tests conducted by varying capacitor charge voltage, the parts shown in Fig. 9 were obtained. It was observed some tendency of wrinkling (Fig. 9d) around of the circular window of the metal can.

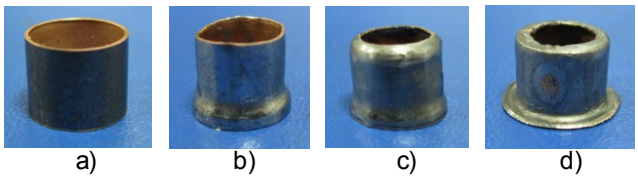

Fig. 9. Experimental results for different charging voltages: a) Undeformed (workpiece); b) 3 kV; c) 4 kV; d) 5 kV.

For further study, more tests need to be done changing the workpiece material and wall thickness, as well as axial position adjustment of the workpiece relative to solenoidal coil.

5. Conclusions

In this work, electromagnetic forming process is used as a method for obtaining of a TO-39 metal can. In the development of this new forming method for metal cans, in which are enclosed optoelectronic components (photodiodes, phototransistors), FEM simulation was utilized. The conclusions are as follows:

- The relative positioning between workpiece, mandrel and coil is very important in order to obtain necessary form and dimensions for final part;
- FEM simulation provides very useful information for tools design (coil and mandrel), which otherwise require costly trial and error experimental tests;
- Also, from FEM simulation are obtained the main working parameters, e.g. discharging energy;
- The main advantage of using electromagnetic forming instead of classical deep-drawing process

for these metal cans, results from the fact that material losses are entirely eliminated (the workpiece is cut-off from tube and material volumes of workpiece and final part are equal);
- The energy consumed per part by this method is almost 50 times smaller than that required in classic methods;
- Electromagnetic forming seems to be a proper method for obtaining such type of parts, but more experimental tests needs to be done with different tube materials and thickness.

References

[1] M. Kleiner, C. Beerwald, W. Homberg, Ann. CIRP, **54**(1), 225 (2005).
[2] H. Zhang, M. Murata, H. Suzuki, Journal of Materials Processing Technology, **48**, 113 (1995).
[3] S. H. Lee, D. N. Lee, Journal of Materials Processing Technology, **57**, 311 (1996).
[4] J.D. Thomas, M. Seth, G.S. Daehn, J.R. Bradley, N. Triantafyllidis, Acta Materialia, **55**, 2863 (2007).
[5] Z. Li, C. Li, H. Yu, Z. Zhao, Trans. Nonferrous Met. Soc. China, **17**, 705 (2007).
[6] C. Shin, H. H. Jin, J. G. Lee, D.-J. Lee, C.-K. Rhee, J.-H. Hong, Metals and Materials International, 14(1), 91 (2008).
[7] J. Shang, S. Hatkevich, L. Wilkerson, J. Shang, S. Hatkevich, L. Wilkerson 5th International Conference on High Speed Forming, Germany, 2012, p. 83.
[8] C. Karch, K. Roll, Advanced Materials Research, **6-8**, 639 (2005).
[9] H. Yu, C. Li, J. Deng, Journal of Materials Processing Technology **209**, 707 (2009).
[10] H. Yu, C. Li, Journal of Materials Processing Technology, **209**, 1053 (2009).
[11] D. Luca, International Journal of Numerical Modelling: Electronic Networks, Devices and Fields, **25**, 15 (2012).
[13] R. Otin, International Journal of Solids and Structures, **50**(10), 1605 (2013)**.**
[14] Z. F. Wang, F. X. Piao, Z. Y. Wang, J. Z. Cui, M. X. Ma, J. of the Braz. Soc. of Mech. Sci. & Eng., **XXX III**(1), 41 (2011).
[15] A. Vivek, K.-H. Kim, G. S. Daehn, Journal of Materials Processing Technology, **211**, 840 (2011).
[16] P. Gharghabi, P. Dordizadeh B., K. Niayesh, Journal of the Korean Physical Society, **59**(6), 3560 (2011).
[17] S. Rajiv, K. Shanmuga Sundaram, C. Narendran, Procedia Engineering, **38**, 2520 (2012).
[18] H. Jiang, C. Li, H. Yu, Z. Zhao, J. Mater. Sci. Technol., **19**(1), 129 (2003).
[19] V. Schulze, P. Barreiro, D. Löhe, Advanced Materials Research, **10**, 79 (2006).
[20] S. S. Brar, D. Pathak, A. Mahajan, R. K. Bedi, J. Optoelectron. Adv. Mater, **14**(7-8), 613 (2012).
[21] S. Sathish, B. Chandar Shekar, J. Optoelectron. Adv. Mater,**15**(3-4), 139 (2013).
[22] G. Zhang, Y. Zeng, Y. Yan, Y. Leng, J. Optoelectron. Adv. Mater, **16**(7-8), 919 (2014).
[23] K. S. Karimov, S. A. Moiz, M. Mahroof Tahir, N. Ahmed, R. Tariq, S. Z. Abbas, Q. Zafar, J. Optoelectron. Adv. Mater,**16**(11-12), 1430 (2014).
[24] M. Lax, D. F. Nelson, Physical Review B, **13**(4), 1777 (1976).
[25] P. P. Silvester, R. L. Ferrari, Finite Elements for Electrical Engineers, Cambridge University Press, Cambridge (1987).
[26] J.C. Maxwell, A Treatise on Electricity and Magnetism, Vol. II, Clarendon Press, Oxford (1873).
[27] http://www.jedec.org/sites/default/files/.../to-039.pdf
[28] A.G. Mamalis, D.E. Manolakos, A.G. Kladas, A.K. Koumoutsos, Applied Mechanics Reviews (ASME), **57**(4), 299 (2004).

* Corresponding author: dluca@tuiasi.ro